Environmental Science and Pollution Research (2020) 27:18972–18984
https://doi.org/10.1007/s11356-018-3250-1

NANOTECHNOLOGY, NANOPOLLUTION, NANOTOXICOLOGY AND NANOMEDICINE (NNNN)

Evaluation of phytotoxicity, cytotoxicity, and genotoxicity of ZnO nanoparticles in *Vicia faba*

Mohamed S. Youssef[1] · Rabab M. Elamawi[2]

Received: 20 April 2018 / Accepted: 14 September 2018 / Published online: 20 September 2018

Abstract

Due to the accelerating use of manufactured nanomaterials, more research is needed to define their impact on plants. The present investigation aimed at evaluating the effect of different levels (0.0, 10, 25, 50, and 100 mg/L) of ZnO nanoparticles (NPs) on *Vicia faba* during seed germination and seedling establishment. Additionally, *V. faba* root meristems were used as a model to monitor the cytotoxic and genotoxic effects resulting from exposure to ZnO NPs. The influence of ZnO NPs on three isoenzyme systems, peroxidase, α, and β esterase, was also evaluated using native-PAGE. Our results showed that lower concentrations of ZnO NPs (especially 10 and 25 mg/L) enhanced seed germination and improved seedling growth, while higher concentrations (100 and 200 mg/L) resulted in phytotoxicity. Cytological investigations of ZnO NPs-treated *V. faba* root cells denoted the clastogenic and aneugenic nature of ZnO NPs. Differential increase in mitotic index and significant alterations in cell cycle were observed upon exposure to ZnO NPs. High concentrations of ZnO NPs markedly induced chromosomal aberration, micronuclei, and vacuolated nuclei formation. Chromosomal breakage, chromosomal bridges, ring chromosomes, laggard chromosomes, and stickiness were also observed at a higher rate. The PAGE analysis showed that ZnO NPs treatments altered the expression patterns of all studied enzyme systems. Collectively, results from this work will help to further understand the phytotoxic effects of nanomaterials.

Keywords Chromosomal aberration · Clastogenicity · Isoenzymes · Nanoparticles · Nanotoxicity · *Vicia faba*

Introduction

In recent years, research on nanoparticles (NPs) has received a lot of attention, due to their attributes and physical characteristics such as small size, shape, and bigger surface area to mass ratio. These prosperities have created a new dimension in current science and technology with their wide-ranging applications in medicine, drug development, agriculture, and many more applications. Conversely, the ability of the NPs to interact with the cell membrane, cross cell barriers, and interact with intracellular molecules poses serious problems and results in genetic toxicity and oxidative stress (Landsiedel et al. 2009; Rico et al. 2011).

ZnO is thought to be a "GRAS" (generally recognized as safe) substance by the FDA (2011). However, the GRAS assignment most usually alludes to materials in the micron to bigger size range, as even these substances when reduced to the nanoscale can develop new actions of toxicity (Rasmussen et al. 2011). Lin and Xing (2007) tested the phytotoxicity of ZnO NPs, Zn^{2+} dissolution from ZnO NPs, and Zn^{2+} from ZnSO4.7H2O on seed germination and root growth of six plant species. Only ZnO NPs displayed phytotoxicity and no marked negative effect on germination and root elongation was noted for the similar concentration of Zn^{2+}. Accordingly, they ascribed the phytotoxicity to nano-ZnO. Consequently, a detailed evaluation of ZnO NPs toxicity is needed. However, it is also important to quantify the amount of Zn^{2+} released from a given dose of ZnO NPs.

Nano-ZnO is in the sixth level of eleven highly produced manufactured nanomaterials (MNMs) in decreasing order: carbon black; nano-SiO2, -Al2O3, -TiO2, -CeO2, -ZnO, and -ZrO2, carbon fiber, nano-CuO, and -Ag (Holden et al. 2014). ZnO NPs have many uses, including application in sunscreens, personal

Responsible editor: Philippe Garrigues

✉ Mohamed S. Youssef
m.s.gad@sci.kfs.edu.eg

[1] Botany Department, Faculty of Science, Kafrelsheikh University, Kafrelsheikh 33516, Egypt

[2] Rice Pathology Department, Plant Pathology Research Institute, Agricultural Research Center, Sakha, Kafrelsheikh 33717, Egypt

care, and paints (Osmond and McCall 2010). Additionally, they have been applied in medicine and biology, where they have been assessed for tumor cell annihilation and delivery mediator for drug treatment (Rasmussen et al. 2011). ZnO NPs could reach to plants either intentionally or unintentionally. Intentional exposure includes their direct application as fertilizer (Liu and Lal 2015) and as fungicides because of their antifungal activity (He et al. 2011). While unintentional exposure could occur through the accidental release of ZnO NPs into the air, water, and soil because of excess production, use, and disposal. Thus, the ecological risk of ZnO NPs is an important issue.

Recently, phytotoxicity of ZnO NPs on seed germination and root growth has been documented in lettuce, radish, cucumber (Lin and Xing 2007), wheat (Du et al. 2011), cabbage (Pokhrel and Dubey 2013), rice (Chen et al. 2015), cucumber (Zhang et al. 2015b), black mustard (Zafar et al. 2016), and corn (López-Moreno et al. 2017). Additionally, Wang et al. (2018) reported a significant reduction in the dry weights of shoots and roots of maize after ZnO NPs treatment. Also, ZnO NPs caused genotoxicity in broad bean (Manzo et al. 2011). Studies in ryegrass revealed that besides decreasing biomass, exposure of ZnO NPs resulted in shriveled root tips and epidermis, and distorted cortical cells (Lin and Xing 2008). Brunner et al. (2006) referred the toxicity of metal oxide NPs to three different mechanisms: (i) dissolution of corresponding metal ion; (ii) surface modification and interaction with media; (iii) disruption biomolecules. On the other hand, ZnO NPs have been reported to enhance seed germination and promote root and shoot length in different plant species including peanut (Prasad et al. 2012), cluster bean (Raliya and Tarafdar 2013), wheat (Ramesh et al. 2014), and maize (Estrada-Urbina et al. 2018).

To date, the prospect of the harmful health effects of nanoparticles (NPs) is inadequately comprehended and require further investigation. A limited number of studies have been directed on the genotoxic impacts of NPs on plant systems. Studies on the assessment of toxicity of zinc NPs on palatable plants are meager (Patlolla et al. 2012; Ma et al. 2015; Taranath et al. 2015). Plant bio-systems have been widely used as a genotoxicity module in evaluating the potential risks and detection of environmental mutagens due to their availability all over the year, fast, simple, inexpensive, efficient, and reliable characters. Plants with low numbers of chromosomes have been considered to be admirable cytogenetic systems with a wide range of genetic endpoints, from gene mutation to chromosome abnormalities, variations in ploidy levels, and DNA damage (Kumari et al. 2009). *Vicia faba* has six pairs of relatively large chromosomes that are great for surveying cyto-genotoxicity. In addition, it has the advantage of being inexpensive and easy to grow and handle. The *V. faba* root meristem chromosomal mutation assay is a well-known plant bioassay approved by the International Programme on Chemical Safety (IPCS, WHO) and the United Nations Environment Programme (UNEP) as an effective and standard test for the chemical screening and in situ surveillance for genotoxicity of environmental elements. The mitotic root meristems of *V. faba* have in fact been used as pioneer cytogenetic materials for assessing chromosomal mutations since the 1920s (Ma 1982; Kanaya et al. 1994).

An examination of the mitotic index (MI), phase index, chromosomal aberrations (CA), and micronuclei (MN) induction would thus be able to give a confirmation to the cytotoxicity and genotoxicity of NPs in plants. Previous studies reported a decrease in MI values in the root tips of *Allium cepa* and *V. faba* with increasing concentration of ZnO NPs and exposure duration (Kumari et al. 2011; Taranath et al. 2015; Ghosh et al. 2016). Micronuclei are a significant indicator of either numerical or structural chromosomal aberrations and are known to be incited by an assortment of mutagenic and carcinogenic substances. The MN test can efficiently detect both effects: clastogenic and aneugenic (Krishna and Hayashi 2000). Clastogenicity (structural chromosomal breakage) and aneugenicity (aneuploidy or chromosomal numerical alterations) are caused by different actions of a chemical or its metabolites on the genome; the earlier is triggered mainly by interaction with DNA and chromatin, while the latter is because chromosomal nondisjunction produced by interfering with spindle function (Styles et al. 1997). Micronucleus assay is frequently used as a genotoxicity test on nanomaterials (Landsiedel et al. 2009).

Proteins are the main products of active structural gene expression; their size and amino acids sequence are the direct results of expression processes. Consequently, any detectable change in protein-banding pattern brought by any mutagen is considered a mirror for genetic variations (Hamoud et al. 2005). Based on this notion, alteration of protein/isoenzyme profile could be useful for exploring mutagenic potentiality of pollutants or chemicals as well as nanomaterials. Plant esterases had been reported as good bioindicators to detect the presence and toxicity of residues of topically applied insecticides in agriculture (Carvalho et al. 2003) and could be valuable for monitoring pollutants in the environment. So, in the present investigation, we studied the expression patterns of α and β esterases to investigate the toxicity of ZnO NPs at the biochemical level.

From the literature cited herein, it is apparent that there is a great debate on the phytotoxic effects of ZnO NPs, and whether their utilization should be restricted or encouraged given their effects on plant morphogenesis. The present work aims at clarifying some of these issues through the evaluation of ZnO NPs effects on morphology, cytology, and biochemistry of *V. faba.*

Materials and methods

Preparation and characterization of ZnO nanoparticles

The ZnO nanopowder (M K Impex Corp Mississauga, Canada) with primary diameter of 30 nm was suspended

directly in de-ionized water (DI-water) to prepare a stock solution at 500 mg/L concentration, and dispersed by ultrasonic vibration (130 W, 20 kHz) for 30 min to avoid aggregation of NPs. Five different concentrations of ZnO NPs (10, 25, 50, 100, and 200 mg/L) were freshly prepared. Suspensions were continuously mixed to prevent NPs sedimentation using a magnetic stirrer before use.

The ZnO NPs were characterized by transmission electron microscope (TEM) using a JEOL JEM-2100 electron microscope and dynamic laser light-scattering method (DLS). The particles size distribution and zeta potential in liquid suspension of ZnO NPs (100 mg/L) were both measured at 25 °C using Zetasizer Nano-ZS90 (Malvern Instruments, Worcestershire, UK). Dispersion status was described by the intensity-weighted hydrodynamic average diameter (Z-average) and polydispersity index (PdI), which reflect the broadness of the size distribution. The measurements were taken in triplicate and recorded as the mean ± standard deviation.

Direct in situ measurement of zinc ions dissolution from ZnO NPs using anodic stripping voltammetry

In the present study, anodic stripping voltammetry (ASV) with a hanging mercury drop electrode was applied to directly measure the concentration of dissolved zinc ions in the investigated ZnO NP suspensions, without separation of the ZnO NPs from the aqueous phase according to Jiang and Hsu-Kim (2014) with slight modifications. Dissolved Zn was quantified immediately after preparation of ZnO NP suspensions (0 h values) and after 48 h of ZnO NPs dispersion, to ensure the solutions had reached a steady state of dissolution as well as aggregation. Used solutions of Hg^{2+} and Zn^{2+} were prepared by direct dilution from 1000 mg/L standard solution (Merck—for ICP and spectroscopic measurements) to the required concentrations using de-ionized water. Hydrochloric acid (Aldrich) of purity 99.999% was diluted with de-ionized water and used as a supporting electrolyte for mercury film deposition. Britton-Robinson universal buffer of pH 7.5 was prepared from acetic, phosphoric, and boric acids of analytical grade in de-ionized water and used as supporting electrolyte in voltammetric measurements.

All voltammetric measurements were performed with Princeton Applied Research (PAR, Oak Ridge, TN, USA) Potentiostats Model VersaSTAT. A voltammetric cell consisting of a K0264 micro-cell with a glassy carbon milli-electrode (PAR—G0229, 3 mm in diameter), an Ag/AgCl/saturated KCl reference electrode (PAR—K0265), and a platinum wire counter electrode (PAR—K0266) were used. The data were treated through a PC connected to the potentiostat and loaded with the (PAR—VersaStudio 2.43.3) software.

Biological materials

Seeds of *Vicia faba* cv. Sakha 3 were obtained from the Agriculture Research Center, Kafrelshiekh, Egypt.

Evaluation of phytotoxicity of ZnO NPs using germination test and seedling vigor

Healthy and uniform *V. faba* seeds were immersed in a 10% sodium hypochlorite solution for 10 min to ensure surface sterility, followed by rinsing three times with distilled water. The seeds were allowed to germinate at 25 ± 2 °C on filter papers saturated with tested concentrations of ZnO NPs or distilled water as a control. Three replicates with 10 seeds/dish per each treatment were used. Germination percentage was calculated after 10 days of treatment.

Seedling vigor parameters including: shoot height, root length, and seedling vigor index (VI) were recorded after 20 days. VI was calculated according to Dhindwal et al. (1991).

Evaluation of cytotoxicity and genotoxicity of ZnO NPs

V. faba seeds were allowed to germinate on filter papers moistened with distilled water till root length reached about 1 cm. Then roots were placed in contact for 24 h with different concentrations of ZnO NPs (10, 25, 50, 100, and 200 mg/L) and with distilled water as a control. Three replicates were used for each treatment. The roots were then fixed in ethanol: acetic acid (3:1) for 24 h, followed by hydrolysis with 1 M HCl for 9 min in a water bath at 60 °C. The roots were stained with Schiff reagent for 2 h, followed by slides preparation by squashing well-stained root tips with 45% acetic acid under a cover glass. The analyses were performed with an optical microscope at × 40 magnification, considering the total number of cells, the number of cells in the division, and the number of alterations. Different phases of mitosis were counted to calculate the mitotic index (MI, the number of cells in division/total number of cells counted), phase indices (PI, number of cells at each stage/ number of cells in division), and total chromosomal abnormality percentage (CA, the number of cells with chromosomal alterations/number of cells in division).

Micronuclei (MN) with a diameter not exceeding one third of the main nucleus were counted. The frequency of MN was expressed as the number of cells with micronuclei per 1000 scored interphase cells (Hu et al. 2017). Percentage of cells with vacuolated nuclei was calculated from the interphase. At least a total of 2000 cells were counted per each biological replicate for each treatment.

Evaluating the impact of ZnO NPs on isoenzyme expression pattern using native PAGE analysis

V. faba seeds were allowed to germinate and grow for 2 weeks on filter papers moistened with studied ZnO NPs concentrations. Leaves from at least three different plants per each treatment were grinded in liquid nitrogen to a fine powder. Total native protein was extracted by mixing 100 mg fine powder with 1000 μL sodium phosphate buffer, pH value of 7.2 for 1 h at room temperature with moderate vortexing for 10 to 15 s every 10 min. The mixture was centrifuged for 20 min at 15000 rpm under cooling. The supernatant was kept at − 20 °C until use. Native proteins were separated by native polyacrylamide gel electrophoresis according to Laemmli (1970). Then, the gels were stained with specific substrates for each enzyme system. The peroxidase (POX), α, and β esterase (Est) enzymes of treated plants were examined as described by Soltis et al. (1983).

In case of peroxidase, bands were detected by incubating the gel in 0.05 M acetate buffer (pH 5.0 ± 0.1) containing 65.0 mg ơ-dianisidine dissolved in 5 ml ethanol. Two milliliters of 0.1 M $CaCl_2$ were added as co-enzyme. Finally, 2 ml of H_2O_2 (3% *V/V*) were added as the substrate. Gels were incubated in a refrigerator until bands appeared. For visualization of isoesterases activity, the gels were incubated at room temperature for 1 h in 100 ml of 0.1 M sodium phosphate (pH 6.0 ± 0.1), containing 0.02 g α-naphthyl acetate or 0.02 g β-naphthyl acetate dissolved in 1 ml acetone each, as substrate, and 0.15 g fast blue BB. The enzyme and substrate react to produce specifically colored stained bands. All reactions were performed no less than twice, and just stable products were scored and photographed (Fig. 6).

For isozyme data analysis, relative mobility (Rf) of bands was calculated. When a band is expressed independently, it was considered as an expression of a single isoenzyme of the investigated enzyme system. The isoenzymes were numbered in sequence starting from the cathode, according to their increase in negative charge (Fig. 6).

Statistical analysis

The significance of differences among means was carried by Duncan's multiple range tests at $P < 0.05$. The results are expressed as mean ± SD of three replicate per each treatment and were subjected to one-way analysis of variance (ANOVA) using SPSS v.17 (SPSS, Chicago, USA).

Results

Characterization of ZnO nanoparticles

Transmission electron microscopy showed that the average size of ZnO NPs was 30 nm which, is fitted with the primary diameter according to the manufacturer. The particles were nearly spherical (Fig. 1A).

The analysis software of DLS provided the mean size, size distribution, and polydispersity index (PdI) of the ZnO NPs suspension. DLS displayed Z-average particle hydrodynamic diameter of 79.6 ± 5 nm. It was about three times larger than the primary diameter reported by the manufacturer and the diameter recoded using TEM. The PdI value was 0.251 showing a narrow particle size distribution (Fig. 1B). The zeta potential average was 16.4 ± 3.9 mV (Fig. 1C) indicating moderate stability and dispersion of ZnO NPs in the solution.

Anodic stripping voltammetry measurements of zinc ions dissolution

Stripping analysis is an extremely sensitive electrochemical technique for measuring trace metals (Jiang and Hsu-Kim 2014). Its remarkable sensitivity is attributed to the combination of an effective preconcentration step with advanced measurement procedures that generates an extremely favorable signal: background ratio. Since the metals are preconcentrated into the electrode by factors of 100–1000, detection limits can be in concentration levels down to 10^{-10} M. Therefore, anodic-stripping voltammetry in square-wave mode (SW-ASV) was used for determination of free zinc metal ions in the investigated suspensions of ZnO nanoparticles at a mercury film electrode in Britton-Robinson buffer of pH 7.5 immediately after dispersion of ZnO NPs (Fig. 2A) and after 48 h from dispersion (Fig. 2B). A well-defined anodic peak corresponding to zinc was obtained at − 1.14 V using accumulation time (t_{acc}) of 30 s at accumulation potential (E_{acc}) of − 1.5 V. The peak heights corresponding to the free Zn^{2+} in the investigated solutions of ZnO NPs after 48 h from dispersion showed a notable decrease to about its half values compared with those of solutions immediately after dispersion (Fig. 2A, B). Voltammetric Zn^{2+} peaks of 25 and 10 mg/L suspensions completely vanished after 48 h indicated that the concentration of free Zn^{2+} in these suspensions was too low to be detected. Table 1 showed the concentrations of the free Zn^{2+} dissolution in the suspensions under investigation estimated by standard addition method. Zinc ion dissolution from ZnO NPs was concentration dependent. A remarkable decrease in the free Zn^{2+} concentration in the studied ZnO NPs suspensions was detected after 48 h of preparation. The highest value of released Zn^{2+} (1.103 ± 0.11 mg/L) was recorded for 200 mg/L ZnO NPs suspension immediately after preparation, while the lowest value (0.058 ± 0.01 mg/L) was recorded for 50 mg/L ZnO NPs suspension after 48 h from dispersion.

Effect of ZnO NPs on germination and seedling vigor

The effect of ZnO NPs on germination and seedling vigor of *V. faba* cv. Sakha 3 is shown in Fig. 3. Germination was

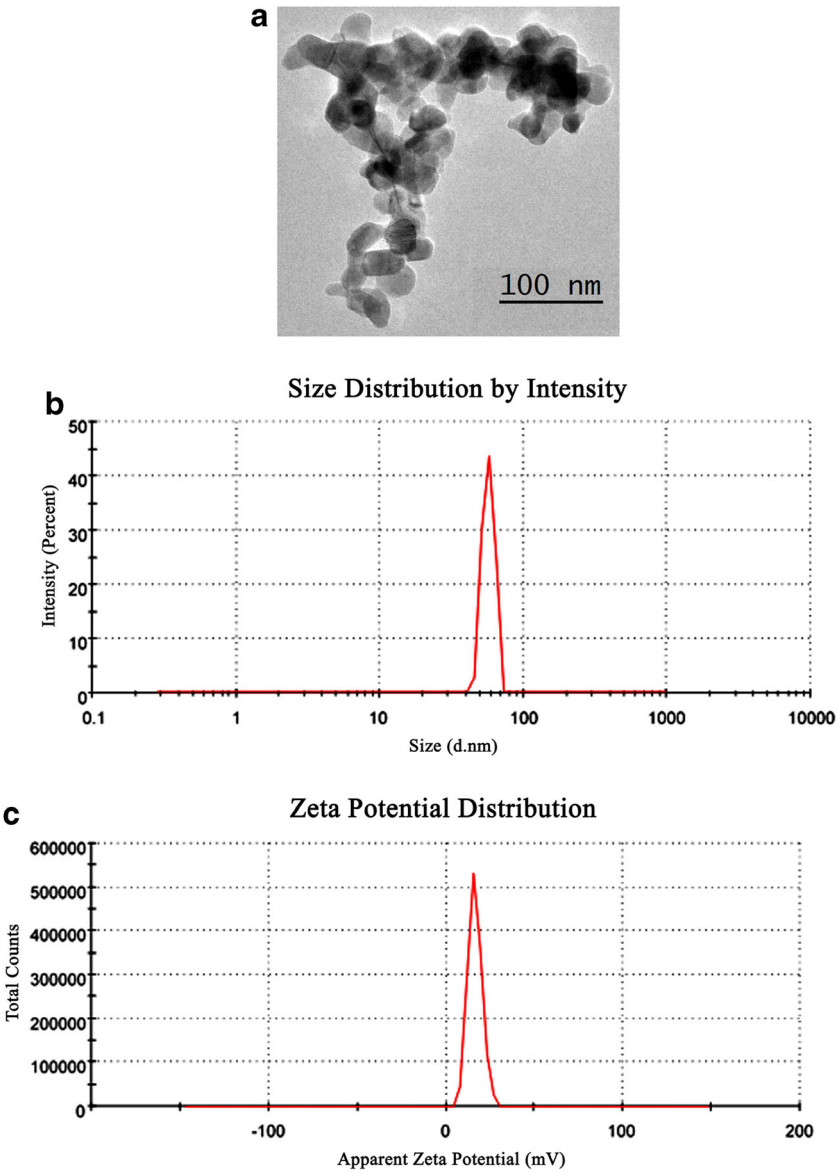

Fig. 1 Characterization of ZnO nanoparticles. (A) Transmission electron microscopy image, (B) particle size distribution measured by dynamic light-scattering technology, and **c** zeta potential of ZnO nanoparticles suspension (100 mg/L)

markedly induced at lower (10–25 mg/L) levels of ZnO NPs (Fig. 3A).

Both root and shoot length were affected by applications of ZnO NPs (Fig. 3B). Root elongation was promoted with increasing levels of ZnO NPs reaching a maximum value of 13 cm with 25 mg/L ZnO NPs and then decreased gradually at higher concentrations. Root elongation was inhibited at the highest level of ZnO NPs tested (200 mg/L). A very similar profile was also observed for shoots exhibiting the most pronounced elongation (about 17 cm) with 25 mg/L ZnO NPs. As for the roots, shoot growth was inhibited when 200 mg/L ZnO NPs concentration was used (Fig. 3B).

The beneficial effects of lower-medium levels of ZnO NPs on seedling establishment were also confirmed using the vigor index, which reached a maximum value at 25 mg/L ZnO NPs (Fig. 3C), corresponding to a 100% increase relative to control conditions (Fig. 3D). At higher ZnO NPs levels the vigor index gradually declined in a trend similar to that observed for the shoot and root growth (compared Fig. 3B–D). At a morphological level, plants appeared taller when treated with 25 mg/L ZnO NPs (Fig. 3E). At the highest ZnO NPs levels (100 and 200 mg/L), the root tips exhibited a dark coloration denoting signs of necrosis.

Collectively, these results clearly show the beneficial effects of low-moderate levels of ZnO NPs on plant performance.

Cytotoxic and genotoxic effect of ZnO NPs

The clastogenic/aneugenic effects of ZnO NPs were assessed on the basis of a chromosome aberration test in *V. faba* root meristems. The MI values, phase index, chromosomal

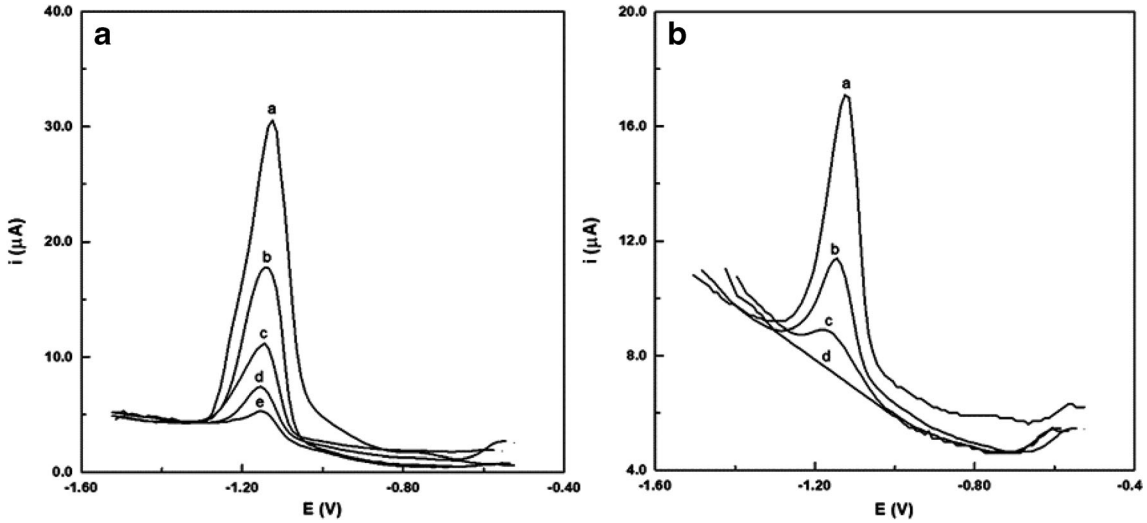

Fig. 2 Square-wave anodic-stripping voltammograms of Zn^{2+} in the investigated solutions of ZnO NPs in Britton-Robinson buffer solution of pH 7.5 (A) Immediately after suspension and (B) after 48 h of suspension; (a) 200 mg/L, (b) 100 mg/L, (c) 50 mg/L, (d) 25 mg/L, and (e) 10 mg/L. Instrumental conditions: frequency (f) = 100 Hz, scan increment (Δs) = 10 mV, and pulse height (a) = 25 mV. Accumulation conditions: potential (E_{acc}) − 1.5 V and time (t_{acc}) = 30 s

aberration, MN frequencies, and vacuolated nuclei frequency are given in Fig. 4.

In the present investigation, all tested concentrations of ZnO NPs increased the MI values in comparison to the control treatment (Fig. 4A). This increase was highly significant when treating root cells with 10 and 25 mg/L ZnO NPs. The highest MI value (13.75) was recorded at 10 mg/L ZnO NPs.

With the exception of 10 mg/L ZnO NPs, all levels of nano ZnO altered the cycle of the meristematic cells (Fig. 4B). While no differences were observed for the prophase stage, an increase in metaphase stage was recorded. Treatments of 50 and 100 mg/L ZnO NPs increased the anaphase stage but decreased the telophase frequency (Fig. 4B).

Exposure of *V. faba* roots tips to ZnO NPs increased the percentage of chromosomal aberration in a concentration-dependent fashion (Fig. 4C). Aberrations, such as chromosomal breakage at metaphase and anaphase (Fig. 5A, B respectively) as well as anaphasic and telophase bridges (Fig. 5C, D respectively) and ring chromosomes (Fig. 5E) were observed. Laggard chromosomes at ana-telophases (Fig. 5F, G) and micronuclei at telophase (Fig. 5H) were also recorded. The presence of sticky chromosomes was observed at different stages of mitosis (Fig. 5I, J).

Micronuclei (MN) frequency was also affected by ZnO NPs, with a gradual increase with the exception of 50 mg/L ZnO (Fig. 4D). Furthermore, the higher concentration of ZnO NPs (100 and 200 mg/L) induced vacuolation of nuclei (Fig. 5K), where the nucleus of the cell showed non-stainability or granulation of chromatin. The highest ratio of vacuolated nuclei was recorded for 200 mg/L treatment. Pycnotic cells with smaller condensed nuclei and vacuolated cytoplasm were also observed with the highest concentration treatment) Fig. 5L).

Table 1 Dissolved Zn^{2+} concentration in ZnO NPs suspensions, as quantified by AVS immediately after preparation (time 0 h) and after 48 h.

ZnO NPs concentration (mg/L)	Concentration of free Zn^{2+} (mg/L)	
	Time 0 h	After 48 h
200	1.103 ± 0.11	0.403 ± 0.05
100	0.598 ± 0.05	0.166 ± 0.02
50	0.331 ± 0.07	0.058 ± 0.01
25	0.186 ± 0.03	*
10	0.097 ± 0.02	*

*Under detection limit

The values represent mean and standard deviation (SD) of three measurements

Impact of ZnO NPs on isoenzyme expression pattern

The isoenzyme expression banding patterns of peroxidase, α esterase, and β esterase enzymes generated from the leaves of *V. faba* seedling are shown in (Fig. 6). Generally, ZnO NPs treatments altered the expression patterns of all studied enzyme systems. The expression pattern of POX revealed a total of four isoforms. Interestingly, the lowest applied concentration of ZnO NPs (10 mg/L) induced the expression of three isoforms, while other treatments induced only two isoforms with lower expression compared to control (Fig. 6A).

For α esterase, a differential expression across the treatments was observed (Fig. 6B). The α esterase profile in treated *V. faba* showed a total of seven isoforms, from which only three isoforms (II, VI, and VII) were expressed in control with a considerable degree of intensity. Exposure to ZnO NPs-

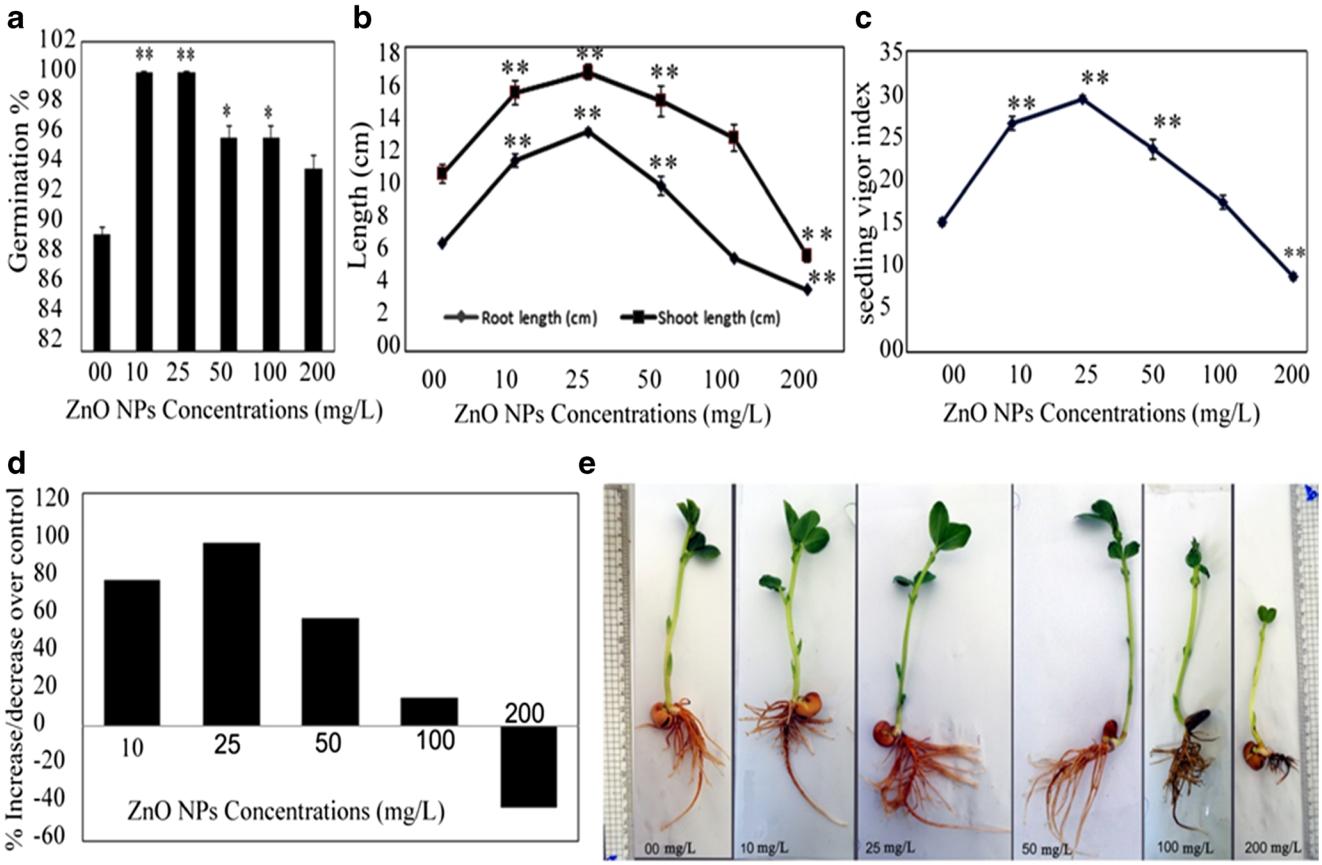

Fig. 3 Effect of different concentrations of ZnO nanoparticles on *Vicia faba* cv. Sakha 3. (A) Germination %, (B) root length (cm), shoot length (cm), and seedling vigor index. (C) Increase/decrease over control related to seedling vigor. (D) Morphological characteristics of the treated plants

induced expression of new isoforms (I, III, IV, and VII) and disappearance of one isoform (VI) (Fig. 6B).

Three isoforms of β esterase were detected for treated *V. faba*. ZnO NPs at 10, 25, and 200 mg/L induced the expression of β Est I while inhibiting that of β Est II. Interestingly, the 50 mg/L ZnO NPs concentration inhibits β Est production as only one isoform (β Est III) was detected with notably decreased band intensity compared to untreated control and other treatments (Fig. 6C).

Discussion

The impact of ZnO NPs on plant growth depends on the size, shape, and the applied concentration of ZnO NPs, as well as the plant species. Nanotoxicity of several nanomaterials to plants at the physiological level has been demonstrated in many studies, resulting in root length inhibition, biomass decrease, altered transpiration rate, and plant developmental delays (Ma et al. 2015). Our results showed that lower concentrations (10 and 25 mg/L) of ZnO NPs enhanced seed germination (Fig. 3A) and promoted root and shoot growth elevating seedling vigor (Fig. 3B, C). Conversely, higher ZnO NPs concentrations (100 and 200 mg/L) exhibited phytotoxicity, significantly inhibited seedling growth (Fig. 3C), and induced browning of roots (Fig. 3D). In agreement with our results, Upadhyaya et al. (2017) documented an enhancement in the germination of rice seeds treated with Zn NPs. Similarly, germination of cucumber seeds increased by 10% after exposure to 1600 mg/L of ZnO NPs. However, alfalfa and tomato showed a reduction in their germination percentage by 40 and 20% respectively (De Rosa et al. 2013). Lin and Xing (2007) reported that nano-Zn and nano-ZnO inhibited seed germination of ryegrass and corn while, not affecting seed germination in radish, rape, lettuce, and cucumber.

To elucidate if the recorded impacts of the investigated ZnO NPs suspensions are due to ZnO NPs or dissolution to Zn^{2+}, the concentration of zinc ions released from ZnO NPs was measured using AVS. Jiang and Hsu-Kim 2014 reported that ASV can measure dissolved Zn^{2+} concentration with sufficient accuracy in the presence of ZnO NPs in the aqueous media. At the beginning of dispersion of ZnO NPs in DI-water (0 h), the high surface energy of the nanoparticles and moderate stability of the suspensions resulted in enhanced dissolution and the dissolved Zn ions concentration increased with increasing the concentration of ZnO NPs (Table 1). By the

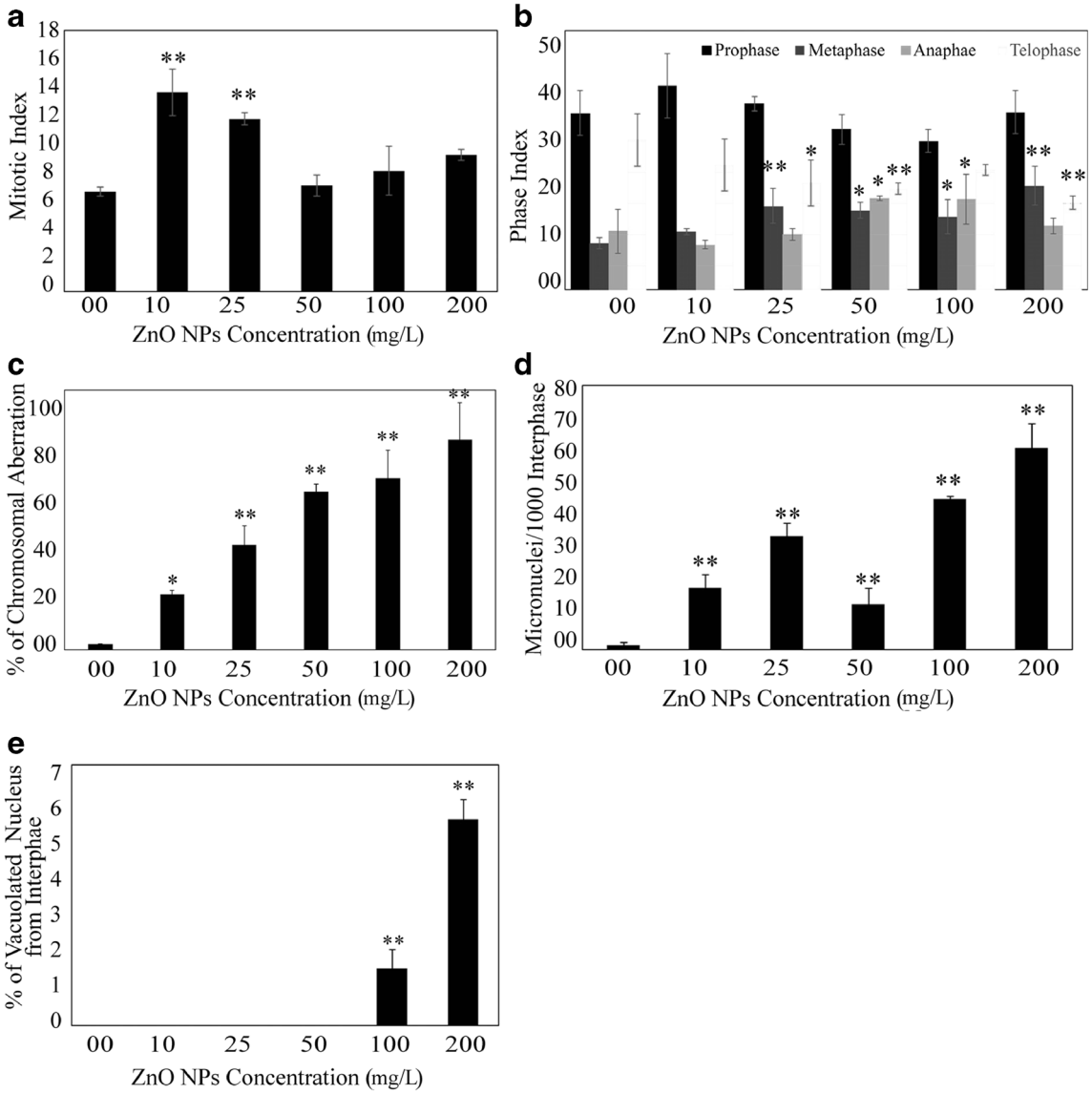

Fig. 4 Cytotoxic effect of ZnO nanoparticles on *Vicia faba* root meristems. (A) Mitotic index value, (B) phase index values, (C) % chromosome aberration, (D) the frequency of micronucleus, (C) % vacuolated nuclei. Each column represents the mean and standard deviation. $*P < 0.05$, $**P < 0.01$ compared with control

time, the dispersed ZnO NPs tend to attract each other forming larger aggregates in order to reduce high surface energy. Aggregation has been shown to decrease the rate of dissolution (Rupasinghe 2011). The recorded decline in Zn^{+2} concentration after 48 h of ZnO NPs dispersion might be due to the aggregation and sedimentation processes. Additionally, adsorption of Zn^{+2} on the surface of ZnO NPs might also lead to the decrease in the free Zn^{+2}. Fatehah et al. (2014) suggested that the adsorption of zinc species that are present in solution affects the sign and the magnitude of the surface charge of ZnO NPs. In the present investigation, the zeta potential average of ZnO NPs was found to be positive 16.4 ± 3.9 mV which supports the above suggestion. Also, the decrease of Zn^{+2} concentration might be due to the precipitation and loss of zinc ions from the dissolved phase in the form of zinc hydroxide according to the following equations:

$$ZnO_{(s)} + H2O \rightarrow Zn^{2+}{}_{(aq)} + 2OH^{-}{}_{(aq)}. \quad \text{(zinc ions dissolution)}$$

$$Zn^{2+}{}_{(aq)} + 2OH^{-}{}_{(aq)} \rightarrow Zn(OH)^{2}{}_{(s)}. \quad \text{(zinc ions sedimentation)}$$

Our results showed that the dissolved Zn^{2+} concentrations in the investigated ZnO NPs suspensions (Table 1) were very small compared to the allowable Zn concentration (5 mg/L) announced by the World Health Organization (WHO 2003). Accordingly, the toxicity reported herein could be ascribed to the nano-ZnO rather than dissolution to zinc ions. This conclusion is completely in agreement with the results obtained by Lin and Xing (2007). They found that only ZnO NPs exhibited

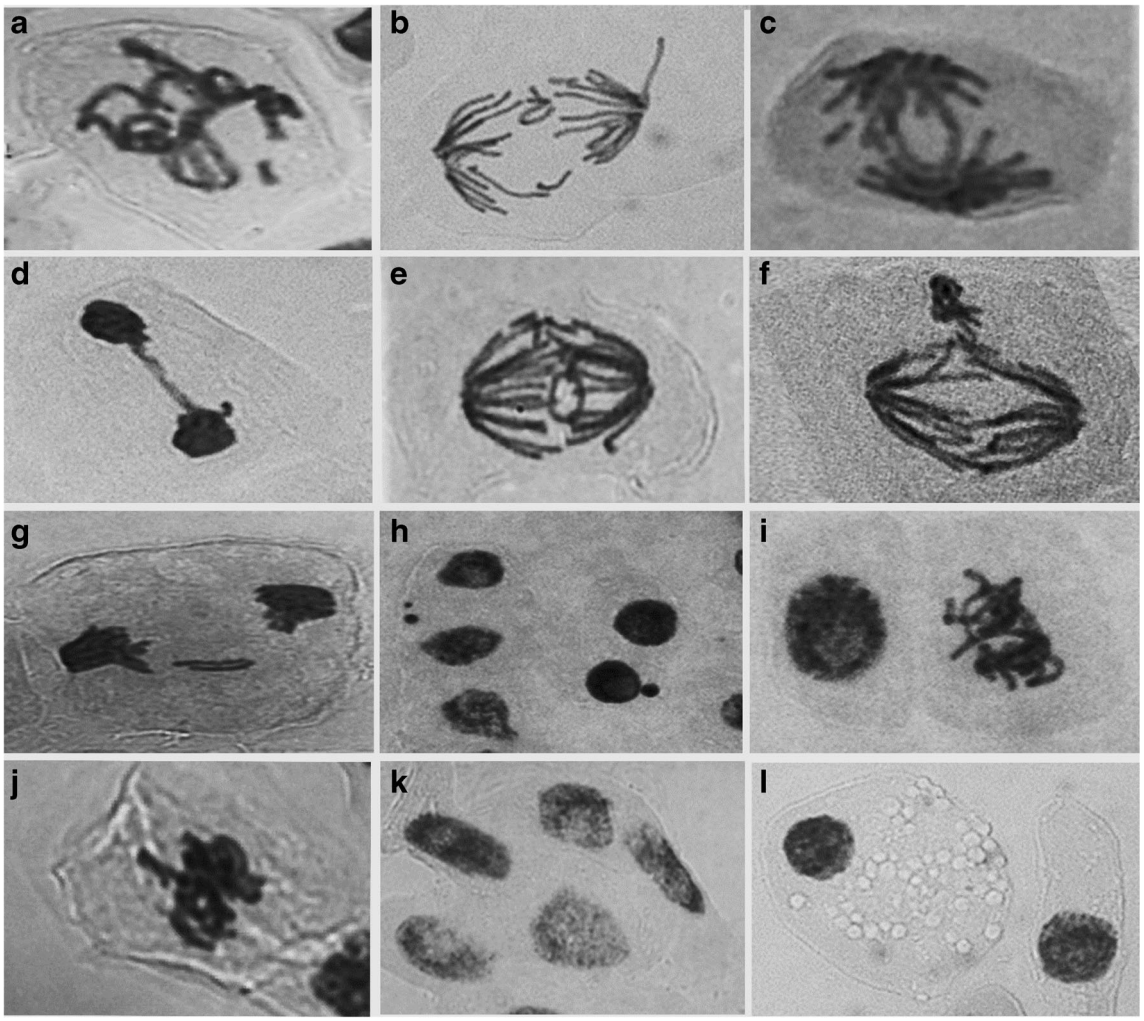

Fig. 5 Induced abnormalities in *Vicia faba* root meristems by different treatments of ZnO nanoparticles. (A) Chromosomal breakage at metaphase. (B) Chromosomal breakage at anaphase. (C) Chromosomal bridge at anaphase. (D) Chromosomal bridge at telophase. (E) Ring chromosome. (F) Laggard chromosome at anaphase. (G) Laggard chromosomes at ana-telophase. (H) Micronucleus at interphase. (I) Sticky prophase. (J) Sticky metaphase. (K) Vacuolated nuclei. (L) Pycnotic cell with vacuolated cytoplasm

phytotoxicity on six plant species, while no marked phytotoxic effects were noted for the similar concentration of Zn^{2+}.

The increment in root and shoot length in the response of studied low ZnO NPs concentrations might be a nutritional behavior of nano zinc oxide or of Zn ions dissolution. Zinc is one of the indispensable micronutrients for the growth of plants. Where zinc ion functions as a cofactor for all six enzyme classes including hydrolases, transferases, oxidoreductases, isomerases, ligases, and lyases (Auld 2001). In addition, Zn provides stabilization of indole-3-acetic acid (Skoog 1940), the predominant auxin in plants, that promotes elongation and cell division. Even though Zn is crucial for sustaining the biological activity of numerous proteins, it causes toxicity when accumulated in excess due to its episodic binding to proteins and consequential displacement of other metal ions including Fe (Lin and Aarts 2012). The inhibitory effect of high levels of ZnO NPs on root elongation reported in our study is in line with the results of Lin and Xing (2007). In their results, 50% root growth inhibitory concentrations (IC_{50}) of nano-ZnO were estimated to be near 50 mg/L for radish, and near 20 mg/L for rape and ryegrass. Also, Lin and Xing (2008) documented a retardation in seedling growth and shorter roots and shoots than the control in ryegrass treated with ZnO NPs, especially at concentrations of ZnO NPs higher than 50 mg/L. These findings are in accordance with those reported herein. In the same line, Chen et al. (2015) reported phytotoxicity of ZnO NPs to rice seedlings in a dose-dependent fashion. They documented a marked reduction in root length, shoot height, and biomass especially with higher than 250 mg/L ZnO NPs. Wang et al. (2018) confirmed that a high dose of ZnO NPs can release bioavailable Zn^{2+} and produce significant toxicity to plants. Jahan et al. (2018) attributed root browning to the adsorption or accumulation of ZnO NPs on the root tips. Manzo et al. (2011) reported that ZnO NPs resulted in higher toxicity in insoluble form towards different terrestrial organisms compared to similar concentrations of zinc in ionic form.

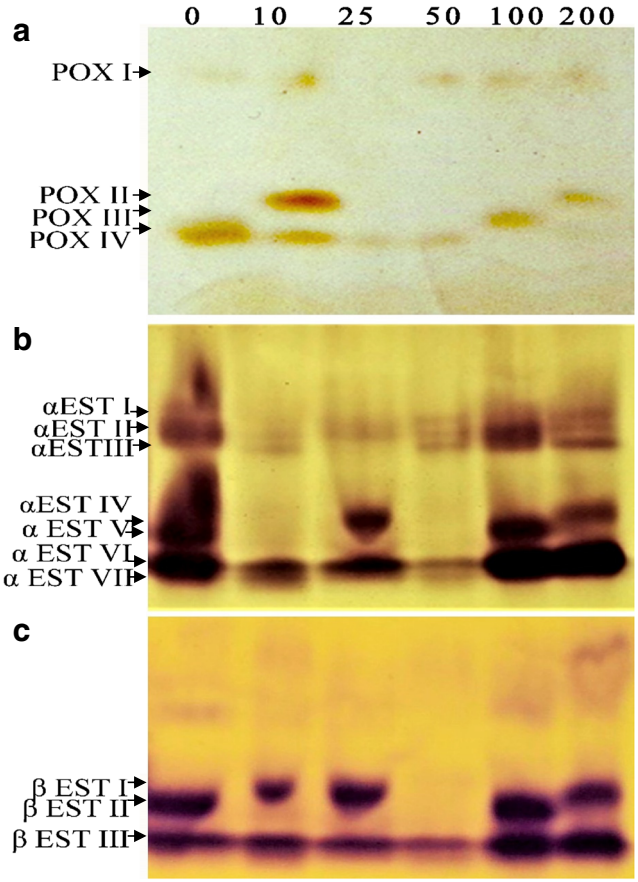

Fig. 6 A zymogram showing the native PAGE patterns of three enzyme systems in *Vicia faba* under the effect of different levels (0–200 mg/L) of zinc oxide nanoparticles. (A) Peroxidase (POX), (B) alpha esterase (α Est), and (C) beta esterase (β Est).

The phytotoxicity of ZnO NPs at higher concentrations could be attributed to their ability to penetrate root and shoot cells and to interfere with the metabolic process. The ability of ZnO NPs to enter plant cells has been reported by many researchers. Lin and Xing (2008) observed the presence of ZnO NPs inside the apoplast and protoplast of endoderms and stele of ryegrass root. Chen et al. (2015) observed ZnO NPs concentrated on the cell wall surface as dark dots in the roots and shoots of rice seedlings under ZnO NPs treatment. Recently, the internalization and presence of ZnO NPs inside plant cells have been confirmed using transmission electron microscope (Zhang et al. 2015a; Ghosh et al. 2016).

The MI is a good indicator of cytotoxicity (Hu et al. 2017). The present investigation showed a differential increase in MI values with different ZnO NPs treatments, with the maximum value recorded for the lower concentration applied (10 mg/L Fig. 4A). However, previous studies reported a decrease in MI values in the root tips of *A. cepa* and *V. faba* with increasing concentration of Zn or ZnO NPs and exposure duration (Kumari et al. 2011; Taranath et al. 2015; Ghosh et al. 2016). The recorded increment in MI value might be due to the cross-talk between Zn^{+2} dissolution from ZnO NPs and auxin. Recently, the cross-talk between Zn and auxin in *Arabidopsis* has been evidenced by Rai et al. (2015). The increased MI with low ZnO NPs concentrations was reflected in the enhancement of root and shoot growth recorded for 10 and 25 mg/L treatments. While, the slight increase in MI observed in case of high ZnO NPs concentrations (100 and 200 mg/L) was not associated with growth improvement but accompanied by growth retardation (Fig. 3B–E), so it might be not due to real cell division but due to accumulation of cells in certain stages and prolonged phases than normal.

All the studied ZnO NPs concentrations significantly altered cell cycle, except the lowest applied concentration (10 mg/L). Metaphase and anaphase were the most sensitive stages to ZnO NPs exposure. The same trend of our results was also reported by Yi et al. (2010) upon treating *V. faba* root cells with aluminum (Al). They suggested that the induction of MN results in some dividing cells enter mitosis (M) with DNA damage-causing cell cycle checkpoints defects. Ghosh et al. (2016) suggested that ZnO NPs induce oxidative stress and DNA damage leading to G2/M cell cycle arrest and apoptosis-like cell death.

In the present investigation, ZnO NPs markedly induced chromosomal aberration in a concentration-dependent manner (Fig. 4C). Our results are incongruent with those remarked by Kumari et al. (2011). The recorded aberrations, as chromosomal breakage, ring chromosomes, chromosomal, and chromatin bridges indicate structural chromosomal rearrangements and a potential clastogenic nature of the ZnO NPs. Furthermore, aberrations as laggard chromosomes and micronuclei (Fig. 5F–H) infer aneugenic effects to ZnO NPs and ability to induce aneuploidy. The sticky chromosomes at different stages of mitosis reflect the toxic effect of ZnO NPs, which is generally irreversible, leading to cell death. This could be the cause of the brown color and stunted roots recorded at 100 and 200 mg/L treatments.

The recorded high frequency of MN demonstrates that ZnO NPs are clear clastogenic/genotoxic and cytotoxic agents in *V. faba* root cells. Similar genotoxic effects of ZnO NPs were reported in *A. cepa* and *V. faba* by Ghosh et al. (2016). Genotoxicity of ZnO NPs contaminated soil in *V. faba* root tip cells was previously reported by Manzo et al. (2011) using the micronucleus test. Vacuolated nuclei observed in the treated cells reveal the severe cytological effect of ZnO NPs that may be attributed to a deficit of DNA in the nucleus. The present results are incongruent with those reported by El-Ghamery et al. (2003). In their investigation, Zn^{2+}-induced vacuolated nuclei in root meristematic cells of *Nigella sativa* and *Triticum aestivum*. Extensive vacuolation and the absence of well-organized nuclei were also observed in root cells of *A. cepa* exposed to carbon nanotubes (Ghosh et al. 2015). In the present study, higher concentrations of ZnO NPs induced vacuolation of the cytoplasm (Fig. 5L). Our findings agreed with those of Lin and Xing (2008), they noted, ZnO NPs induced

vacuolation in root cortical cells of ryegrass. Additionally, extensive vacuolation, loss of nuclear organization, ruptured plasma membrane and shrinkage of the protoplast were observed in *A. cepa* root cells exposed to ZnO NPs (Ghosh et al. 2016). Ma et al. (2015) suggested that the formation of highly vacuolated cortical cells is a defense mechanism against abiotic/oxidative stress triggered by NPs exposure, as this organelle is the main storage site for cytotoxic materials. Zheng et al. (2017) stated that vacuolation is associated with programmed cell death. Ghosh et al. (2016) recorded cell death in root cells of *A. cepa* treated with ZnO NPs using Evans blue dye. So, the growth inhibition recorded in our investigation could be attributed to cell death induced by ZnO NPs (100 and 200 mg/L) treatments.

In the present study, observed stickiness and other chromosomal aberration might be attributed to binding of ZnO NPs with DNA and proteins, causing dangerous changes in their physico-chemical properties, chromatin condensation of the nucleus, or formation of inter- and intra-chromatid crosslinks. This suggestion is fortified by (i) the strong binding affinity of ZnO NPs to DNA (Das et al. 2018), (ii) the formation of ZnO NPs complexes with ring N atom or NH site in nucleobases of DNA (Saha and Sarkar 2014), and (iii) the interaction, as well as the formation of bioconjugate of protein and ZnO NPs, reported by Bhunia et al. (2013), who found that ZnO NPs induced structural changes/unfolding of protein.

ZnO NPs treatments altered the expression patterns of all studied enzyme systems. The results indicate that the effect of ZnO NPs differs according to the applied concentration. In the present work, the recorded changes in peroxidase isoenzyme patterns of *V. faba* after exposure to different levels of ZnO NPs suggest that the peroxidase isoenzyme system could be used to evaluate and quantify the effect of nanomaterial stress on plants. This conclusion is in agreement with the results obtained by Radotić et al. (2000), who reported that the peroxidase isoenzyme pattern could be used as a potential biomarker for sublethal metal toxicity as well as monitoring of oxidative stress. The analysis of α- and β-esterase isoenzymes of *V. faba* confirms the metabolic interference of ZnO NPs with lipid metabolism. Induction of new isoforms and disappearance of existing ones had been detected in treated plants. Similar results were recorded by Carvalho et al. (2003). They reported differential expression (i.e., inhibition and induction) of α- and β-esterase isoenzymes in leaves of *Aspidosperma polyneuron* after in vitro exposure to insecticides using native polyacrylamide gel electrophoresis. In the present investigation, the recorded alteration in the electrophoretic pattern of peroxidase and esterase isozymes upon exposure to ZnO NPs might be due to changes in their amino acid sequences because of induced gene mutation. Isozyme analysis using electrophoresis was used as a powerful tool for mutant identification in several studies (Talukdar 2010; El-Mokadem and Mostafa 2014; Mostafa 2015). Our results confirm the valuable application of plant isozymes as bioindicators to detect toxicity and mutagenic potentiality of nanomaterials, as well as monitoring pollutants in the environment.

In conclusion, ZnO NPs can disturb the metabolic process of the cells through the induction of new isozymes or inhibition/down-regulation of others. As documented herein by the recorded alterations in electrophoretic banding patterns of studied enzyme systems. This disruption might be due to the genotoxic effects of ZnO NPs revealed by the induction of chromosomal mutations and micronuclei formation. Or the interference might be at the transcriptional level, translational level, and or at the post-translational level. The latter suggestion could be reinforced by the ability of ZnO NPs to bind with DNA molecule, deoxyribonucleotides, and NH-group of the ribonucleotides (Saha and Sarkar 2014; Das et al. 2018), as well as they can conjugate with proteins causing unfolding and structural changes and loss of protein function (Bhunia et al. 2013).

Conclusion

Low concentrations (10–25 mg/L) of ZnO NPs could be used to improve plant growth. However, higher concentrations (> 50 mg/L) might lead to their accumulation causing phytotoxicity and cyto-genotoxicity. The *V. faba* cytogenetic test could be used for the genotoxicity monitoring of nanoparticles water contamination. Our results confirm the valuable application of plant peroxidase and esterases as bioindicators to detect the presence and toxicity of nanomaterials and could be valuable for monitoring pollutants in the environment. The present investigation will help to further understand phytotoxicity of ZnO NPs and are momentous in terms of its use and disposal. The mutagenic potentiality of ZnO NPs reported herein could be used in future in mutation breeding to improve crop yield and production of new cultivars. Future studies should be directed to phytotoxicity mechanisms, for example, induction of gene mutation and interference with gene expression.

Acknowledgements Authors would express their deep thanks to Dr. Claudio Stasolla and Dr. Robert Hill, University of Manitoba, Canada, for their valuable suggestions in the manuscript, their fruitful revision, and proofreading the article. Authors also thank Dr. Amr M. Beltagi, Kafrelsheikh University, Egypt, for technical support during AVS analysis and interpretation of data.

References

Auld DS (2001) Zinc coordination sphere in biochemical zinc sites. In: Maret W (ed) Zinc Biochemistry, Physiology, and Homeostasis. Springer, Dordrecht, pp 85–127. isbn:978-90-481-5916-1

Bhunia AK, Samanta PK, Saha S, Kamilya T (2013) ZnO nanoparticle-protein interaction : corona formation with associated unfolding. Appl Phys Lett 103:143701–143705

Brunner TJ, Wick P, Manser P, Spohn P, Grass RN, Limbach LK, Bruinink A, Stark WJ (2006) In vitro cytotoxicity of oxide nanoparticles: comparison to asbestos, silica, and the effect of particle solubility. Environ Sci Technol 40:4374–4381. https://doi.org/10.1021/es052069i

Carvalho VM, Marques RM, Lapenta AS, Machado MDFPS (2003) Functional classification of esterases from leaves of Aspidosperma. Genet Mol Biol 26(2):195–198

Chen J, Liu X, Wang C, Yin SS, Li XL, Hu WJ, Simon M, Shen ZJ, Xiao Q, Chu CC, Peng XX, Zheng HL (2015) Nitric oxide ameliorates zinc oxide nanoparticles-induced phytotoxicity in rice seedlings. J Hazard Mater 297:173–182. https://doi.org/10.1016/j.jhazmat.2015.04.077

Das S, Chatterjee S, Pramanik S, Devi PS, Kumar GS (2018) A new insight into the interaction of ZnO with calf thymus DNA through surface defects. J Photochem Photobiol B Biol 178:339–347. https://doi.org/10.1016/j.jphotobiol.2017.10.039

De Rosa G, López-moreno, De Haro D, Botez CE, Peralta-videa JR, Gardea-torresdey JL (2013) Effects of ZnO nanoparticles in alfalfa, tomato, and cucumber at the germination stage: root development and X-ray absorption spectroscopy studies. Pure Appl Chem 85(12):2161–2174

Dhindwal AS, Lather BPS, Singh J (1991) Efficacy of seed treatments on germination. Seedling emergence and vigour of cotton (*Gossypium hirsutum*) genotypes. Seed Res 19:59

Du W, Sun Y, Ji R, Zhu J, Wu J, Guo H (2011) TiO2 and ZnO nanoparticles negatively affect wheat growth and soil enzyme activities in agricultural soil. J Environ Monit 13(4):822

El-Ghamery AA, El-Kholy MA, Abou El-Yousser MA (2003) Evaluation of cytological effects of Zn 2 + in relation to germination and root growth of *Nigella sativa* L. and *Triticum aestivum* L. Mutat Res Genet Toxicol Environ Mutagen 537:29–41

El-Mokadem HE, Mostafa GG (2014) Induction of mutations in *Browallia speciosa* using sodium azide and identification of the genetic variation by peroxidase isozyme. Afr J Biotechnol 13:106–111

Estrada-Urbina J, Cruz-Alonso A, Santander-González M, Méndez-Albores A, Vázquez-Durán A (2018) Nanoscale zinc oxide particles for improving the physiological and sanitary quality of a Mexican landrace of red maize. Nanomaterials 8(4):247–258

Fatehah MO, Aziz HA, Stoll S (2014) Stability of ZnO nanoparticles in solution. Influence of pH, dissolution, aggregation and disaggregation effects. J Colloid Sci Biotechnol 3(1):75–84

FDA (2011) Part 182—substances generally recognized as safe. Food and drug administration, Washington DC Available at: https://www.law.cornell.edu/cfr/text/21/part-182/subpart-I. Accessed 28 March 2011

Ghosh M, Bhadra S, Adegoke A, Bandyopadhyay M, Mukherjee A (2015) MWCNT uptake in *Allium cepa* root cells induces cytotoxic and genotoxic responses and results in DNA hyper-methylation. Mutat Res Fundam Mol Mech Mutagen 774:49–58. https://doi.org/10.1016/j.mrfmmm.2015.03.004

Ghosh M, Jana A, Sinha S, Jothiramajayam M, Nag A, Chakraborty A, Mukherjee A, Mukherjee A (2016) Effects of ZnO nanoparticles in plants: cytotoxicity, genotoxicity, deregulation of antioxidant defenses, and cell-cycle arrest. Mutat Res Genet Toxicol Environ Mutagen 807:25–32. https://doi.org/10.1016/j.mrgentox.2016.07.006

Hamoud MA, El-Shanshoury AR, Al-Sodany YM, Gad El-Karim MS (2005) Genetic diversity among *Ipomoea carnea* jacq. populations from different habitats types in Nile-Delta region of Egypt. Egypt J Exp Biol 1:1–10

He L, Liu Y, Mustapha A, Lin M (2011) Antifungal activity of zinc oxide nanoparticles against *Botrytis cinerea* and *Penicillium expansum*. Microbiol Res 166:207–215

Holden PA, Klaessig F, Turco RF, Priester JH, Rico CM, Avila-Arias H, Mortimer M, Pacpaco K, Gardea-Torresdey JL (2014) Evaluation of exposure concentrations used in assessing manufactured nanomaterial environmental hazards: are they relevant? Environ Sci Technol 48(18):10541–10551. https://doi.org/10.1021/es502440s

Hu Y, Tan L, Zhang S-H, Zuo Y-T, Han X, Liu N, Lu WQ, Liu AL (2017) Detection of genotoxic effects of drinking water disinfection by-products using *Vicia faba* bioassay. Environ Sci Pollut Res 24(2):1509–1517 http://link.springer.com/10.1007/s11356-016-7873-9

Jahan S, Alias YB, Bakar AFBA, Bin YI (2018) Toxicity evaluation of ZnO and TiO2 nanomaterials in hydroponic red bean (*Vigna angularis*) plant: physiology, biochemistry and kinetic transport. J Environ Sci. https://doi.org/10.1016/j.jes.2017.12.022

Jiang C, Hsu-Kim H (2014) Direct in situ measurement of dissolved zinc in the presence of zinc oxide nanoparticles using anodic stripping voltammetry. Environ Sci Processes Impacts 16(11):2536–2544

Kanaya N, Gill BS, Grover IS, Murin A, Osiecka R, Sandhu SS, Andersson HC (1994) *Vicia faba* chromosomal aberration assay. Mutat Res 310:231–247

Krishna G, Hayashi M (2000) In vivo rodent micronucleus assay: protocol, conduct and data interpretation. Mutat Res 455:155–166

Kumari M, Mukherjee A, Chandrasekaran N (2009) Genotoxicity of silver nanoparticles in *Allium cepa*. Sci Total Environ 407:5243–5246. https://doi.org/10.1016/j.scitotenv.2009.06.024

Kumari M, Khan SS, Pakrashi S, Mukherjee A, Chandrasekaran N (2011) Cytogenetic and genotoxic effects of zinc oxide nanoparticles on root cells of *Allium cepa*. J Hazard Mater 190(1–3):613–621. https://doi.org/10.1016/j.jhazmat.2011.03.095

Laemmli UK (1970) Cleavage of structural proteins during the assembly of the head of bacteriophage T4. nature 227(5259):680

Landsiedel R, Kapp MD, Schulz M, Wiench K, Oesch F (2009) Genotoxicity investigations on nanomaterials: methods, preparation and characterization of test material, potential artifacts and limitations-many questions, some answers. Mutat Res Rev Mutat Res 681(2–3):241–258

Lin YF, Aarts MGM (2012) The molecular mechanism of zinc and cadmium stress response in plants. Cell Mol Life Sci 69:3187–3206

Lin D, Xing B (2007) Phytotoxicity of nanoparticles: inhibition of seed germination and root growth. Environ Pollut 150(2):243–250

Lin D, Xing B (2008) Root uptake and phytotoxicity of ZnO nanoparticles. Environ Sci Technol 42(15):5580–5585

Liu R, Lal R (2015) Potentials of engineered nanoparticles as fertilizers for increasing agronomic productions. Sci Total Environ 514:131–139

López-Moreno ML, de la Rosa G, Cruz-Jiménez G, Castellano L, Peralta-Videa JR, Gardea-Torresdey JL (2017) Effect of ZnO nanoparticles on corn seedlings at different temperatures; X-ray absorption spectroscopy and ICP/OES studies. Microchem J 134:54–61

Ma TH (1982) Vicia cytogenetic tests for environmental mutagens. A report of the U.S. environmental protection agency gene-tox program. Mutat Res Genet Toxicol 99(3):257–271

Ma C, White JC, Dhankher OP, Xing B (2015) Metal-based nanotoxicity and detoxification pathways in higher plants. Environ Sci Technol 49(12):7109–7122

Manzo S, Rocco A, Carotenuto R, Picione FDL, Miglietta ML, Rametta G et al (2011) Investigation of ZnO nanoparticles ' ecotoxicological effects towards different soil organisms. Environ Sci Pollut Res 18:756–763

Mostafa GG (2015) Effect of some chemical mutagens on the growth, phytochemical composition and induction of mutations in *Khaya senegalensis*. Int J Plant Breed Genet 9(2):57–67

Osmond MJ, McCall MJ (2010) Zinc oxide nanoparticles in modern sunscreens: an analysis of potential exposure and hazard. Nanotoxicology 4(1):15–41

Patlolla AK, Berry A, May L, Tchounwou PB (2012) Genotoxicity of silver nanoparticles in *Vicia faba*: a pilot study on the environmental

monitoring of nanoparticles. Int J Environ Res Public Health 9(5): 1649–1662

Pokhrel LR, Dubey B (2013) Evaluation of developmental responses of two crop plants exposed to silver and zinc oxide nanoparticles. Sci Total Environ 452:321–332

Prasad TNVKV, Sudhakar P, Sreenivasulu Y, Latha P, Munaswamy V, Raja Reddy K et al (2012) Effect of nanoscale zinc oxide particles on the germination, growth and yield of peanut. J Plant Nutr 35(6): 905–927

Radotić K, Dučić T, Mutavdžić D (2000) Changes in peroxidase activity and isoenzymes in spruce needles after exposure to different concentrations of cadmium. Environ Exp Bot 44(2):105–113

Rai V, Sanagala R, Sinilal B, Yadav S, Sarkar AK, Dantu PK, Jain A (2015) Iron availability affects phosphate deficiency-mediated responses, and evidence of cross-talk with auxin and zinc in Arabidopsis. Plant Cell Physiol 56(6):1107–1123

Raliya R, Tarafdar JC (2013) ZnO nanoparticle biosynthesis and its effect on phosphorous-mobilizing enzyme secretion and gum contents in clusterbean (*Cyamopsis tetragonoloba* L.). Agric Res 2(1):48–57

Ramesh M, Palanisamy K, K B SNK (2014) Effects of bulk & nano-titanium dioxide and zinc oxide on physio-morphological changes in *Triticum aestivum* Linn. J Glob Biosci 3(2):415–422

Rasmussen JW, Martinez E, Louka P, Wingett DG (2011) Zinc oxide nanoparticles for selective destruction of tumor cells and potential for drug delivery applications. NIH Public Access 7(9):1063–1077

Rico CM, Majumdar S, Duarte-Gardea M, Peralta-Videa JR, Gardea-Torresdeay JL (2011) Interaction of nanoparticles with edible plants and their possible implications in the food chain. Agric Food Chem 59:3485–3498

Rupasinghe RP (2011) Dissolution and aggregation of zinc oxide nanoparticles at circumneutral pH; a study of size effects in the presence and absence of citric acid. Master's thesis, University of Iowa, Iowa, IA, USA

Saha S, Sarkar P (2014) Understanding the interaction of DNA – RNA nucleobases with different ZnO nanomaterials. Phys Chem Chem Phys 16:15355–15366

Skoog F (1940) Relationships between zinc and auxin in the growth of higher plants. Am J Bot 27(10):939–951

Soltis DE, Haufler CH, Darrow DC, Gastony GJ (1983) Starch gel electrophoresis of ferns: a compilation of grinding buffers, gel and electrode buffers, and staining schedules. Am Fern J 73(1):9–27

Styles JA, Davies A, Davies R, White IN, Smith LL (1997) Clastogenic and aneugenic effects of tamoxifen and some of its analogues in hepatocytes from dosed rats and in human lymphoblastoid cells transfected with human P450 cDNAs (MCL-5 cells). Carcinogenesis 18(2):303–313

Talukdar D (2010) Allozyme variations in leaf esterase and root peroxidase isozymes and linkage with dwarfing genes in induced dwarf mutants of grass pea (*Lathyrus sativus* L.). Int J Genet Mol Biol 2: 112–120

Taranath TC, Patil BN, Santosh TU, Sharath BS (2015) Cytotoxicity of zinc nanoparticles fabricated by Justicia adhatoda L. on root tips of *Allium cepa* L. a model approach. Environ Sci Pollut Res 22(11): 8611–8617

Upadhyaya H, Roy H, Shome S, Tewari S, M k B, Panda SK (2017) Physiological impact of zinc nanoparticle on germination of rice (*Oryza sativa* L) seed. J Plant Sci Phytopathol 1:62–70

Wang F, Jing X, Adams CA, Shi Z, Sun Y (2018) Decreased ZnO nanoparticle phytotoxicity to maize by arbuscular mycorrhizal fungus and organic phosphorus. Environ Sci Pollut Res 25:23736–23747. https://doi.org/10.1007/s11356-018-2452-x

WHO (2003) Zinc in drinking-water. Background document for preparation of WHO guidelines for drinking-water quality. World Health Organization (WHO/SDE/WSH/03.04/17), Geneva Available at: http://www.who.int/water_sanitation_health/dwq/chemicals/zincsum.pdf

Yi M, Yi H, Li H, Wu L (2010) Aluminum induces chromosome aberrations, micronuclei, and cell cycle dysfunction in root cells of *Vicia faba*. Environ Toxicol 25(2):124–129

Zafar H, Ali A, Ali JS, Haq IU, Zia M (2016) Effect of ZnO nanoparticles on *Brassica nigra* seedlings and stem explants: growth dynamics and antioxidative response. Front Plant Sci 7:535. https://doi.org/10.3389/fpls.2016.00535

Zhang D, Hua T, Xiao F, Chen C, Gersberg RM, Liu Y, Stuckey D, Ng WJ, Tan SK (2015a) Phytotoxicity and bioaccumulation of ZnO nanoparticles in *Schoenoplectus tabernaemontani*. Chemosphere 120:211–219. https://doi.org/10.1016/j.chemosphere.2014.06.041

Zhang R, Zhang H, Tu C, Hu X, Li L, Luo Y, Christie P (2015b) Phytotoxicity of ZnO nanoparticles and the released Zn(II) ion to corn (*Zea mays* L.) and cucumber (*Cucumis sativus* L.) during germination. Environ Sci Pollut Res 22:11109–11117

Zheng Y, Zhang H, Deng X, Liu J, Chen H (2017) The relationship between vacuolation and initiation of PCD in rice (*Oryza sativa*) aleurone cells. Sci Rep 7:41245–41259. https://doi.org/10.1038/srep41245